

## Protective effect of naringenin-7-*O*-glucoside against oxidative stress induced by doxorubicin in H9c2 cardiomyocytes

Xiuzhen Han<sup>1,\*</sup>, Si Gao<sup>1</sup>, Yanna Cheng<sup>1</sup>, Yanzhe Sun<sup>1</sup>, Wei Liu<sup>1</sup>, Linlin Tang<sup>1</sup>, Dongmei Ren<sup>2</sup>

<sup>1</sup>Department of Pharmacology, School of Pharmaceutical Sciences, Shandong University, Ji'nan, China;

<sup>2</sup>Department of Natural Product Chemistry, School of Pharmaceutical Sciences, Shandong University, Ji'nan, China.

### Summary

Doxorubicin (DOX) is one of the most effective chemotherapeutic agents, but cardiotoxicity limits its clinical use. Although the mechanisms are not entirely understood, reactive oxygen species (ROS) and cardiomyocyte apoptosis appear to be involved in DOX cardiotoxicity. Protection or alleviation of DOX cardiotoxicity can be achieved by administration of natural phenolic compounds *via* activating endogenous defense systems and antiapoptosis. Naringenin-7-*O*-glucoside (NARG), isolated from *Dracocephalum rupestre* Hance, could protect from cardiomyocyte apoptosis and induce endogenous antioxidant enzymes against DOX toxicity, but the effects on intracellular ROS generation and cell membrane stability were not demonstrated. In the present study, we investigated the effects of NARG on H9c2 cell morphology, viability, lactate dehydrogenase (LDH) and creatine kinase (CK) leakage, glutathione peroxidase (GSH-Px) activity, intracellular Ca<sup>2+</sup> concentration, and ROS generation. Compared with DOX alone treatment group, the morphological injury of the cells in groups treated by DOX plus NARG was alleviated, cell viability was increased, the amount of released LDH and CK was significantly decreased, the activity of GSH-Px was increased, the content of intracellular Ca<sup>2+</sup> and ROS generation was lowered remarkably. These results suggest that NARG could prevent cardiomyocytes from DOX-induced toxicity by their property of stabilizing the cell membrane and reducing ROS generation.

**Keywords:** Naringenin-7-*O*-glucoside (NARG), doxorubicin (DOX), reactive oxygen species (ROS)

### 1. Introduction

Doxorubicin (DOX) is an anthracycline antibiotic with a broad spectrum of activity and high potency against human malignant neoplasms. However, its clinical use is limited by its severe cumulative dose-related cardiotoxicity (1). It has been suggested that one of the molecular mechanisms responsible for DOX cardiotoxicity is the formation of reactive oxygen species (ROS) (2). The quinone moiety of DOX undergoes a one-electron reduction that is

catalyzed by NAD(P)H reductases to yield a semi-quinone free-radical intermediate, which regenerates the parent quinone by reacting with O<sub>2</sub> to form O<sub>2</sub><sup>-</sup> and H<sub>2</sub>O<sub>2</sub> (3,4). These ROS can then be transformed into the more potent hydroxyl radical HO• which is capable of damaging DNA and proteins, and initiating membrane lipid peroxidation, thus eventually leading to intracellular calcium overload (5), cell death, and cardiac damage. Oxidative stress is now considered a major contributor as a trigger for cardiomyocyte death by apoptosis or cell necrosis (1,6,7). Treatment with antioxidants or natural phenolic compounds has been found to protect against DOX-induced cardiotoxicity (8).

The Chinese traditional medicine *Dracocephalum rupestre* Hance, a wild perennial herb found throughout western China, contains a high content of flavonoids (9), and has offered therapeutic potential for

\*Address correspondence to:

Dr. Xiuzhen Han, Department of Pharmacology, School of Pharmaceutical Sciences, Shandong University, No. 44 West Wenhua Road, Ji'nan, 250012, China.

E-mail: xzyhan@sdu.edu.cn

cardiovascular diseases. In our continuous search for cardioprotective substances from these natural products (10-12), naringenin-7-*O*-glucoside (NARG), a major active flavonoid isolated from *D. rupestris*, has been demonstrated that NARG was able to up-regulate the expression of heme oxygenase-1 (HO-1) and attenuate DOX-induced H9c2 cell apoptosis (13). NARG could prevent cardiomyocytes from DOX-induced toxicity by induction of endogenous antioxidant enzymes *via* phosphorylation of ERK1/2 and nuclear translocation of Nrf2 (14). In the present study, we investigated the effects of NARG on cell membrane stability and ROS generation in H9c2 cardiomyocytes treated with DOX. These results suggest that NARG could prevent cardiomyocytes from DOX-induced injury by their property of stabilizing the cell membrane and reducing ROS generation.

## 2. Materials and Methods

### 2.1. Chemicals and materials

NARG was isolated from *D. rupestris* in our laboratory (15,16) and dissolved in dimethyl sulfoxide (DMSO) for the *in vitro* bioassay. Dulbecco's modified Eagle's medium (DMEM) was purchased from Gibco BRL (Grand Island, NY, USA). Fetal bovine serum was bought from Tianjin TBD Biotechnology Development Center (Tianjin, China). 3-[4,5-Dimethyl-2-thiazolyl]-2,5-diphenyl-2-tetrazolium bromide (MTT) were purchased from Sigma. Lactate dehydrogenase (LDH), glutathione peroxidase (GSH-Px) and creatine kinase (CK) assay kits were from Nanjing Jiancheng Bioengineering Institute (Nanjing, China); the ROS assay kit was from Applygen Technologies Inc. (Beijing, China). Fura-2/AM Ester was provided by Biotium (Hayward, CA, USA).

### 2.2. Cell culture

Rat cardiac H9c2 cells (ATCC Rockville, MD, USA) were cultured in DMEM supplemented with 10% fetal bovine serum, 100 U/mL of penicillin, 100 µg/mL of streptomycin and 5% CO<sub>2</sub> at 37°C. The cells were fed every 2-3 days and subcultured once they reached 70-80% confluence. Cells were plated at an appropriate density according to each experimental design.

### 2.3. Cell treatment with NARG

H9c2 cells were incubated with NARG for 24 h followed by incubation with DOX (10 µM) for another 24 h. After this incubation, cells were harvested after trypsin digestion by centrifugation (1,000 rpm × 5 min) and parameters were measured as described in materials and methods.

### 2.4. *In vitro* cell proliferation

H9c2 cells were seeded in 96-well plates at a density of 5,000 cells/well. Following overnight adherence, cells were incubated with NARG (5, 10, 20, 40, and 80 µM) in DMEM supplemented with 0.5% fetal bovine serum at 37°C for 24 h followed by incubation with/without DOX (10 µM) for another 24 h, and then cell proliferation was determined by MTT assay. Cells were treated with MTT solution (final concentration, 0.5 mg/mL) for 4 h. The supernatants were removed carefully, followed by addition of 100 µL DMSO to each well to dissolve the precipitate. The absorbance was measured at 570 nm in a microplate reader (Synergy HT).

### 2.5. Analysis for generation of ROS

The production of ROS was measured by detecting the fluorescent intensity of an oxidant-sensitive probe CM-H2DCFDA, which is a stable nonfluorescent molecule that passively diffuses into cells, where the acetate can be cleaved by intracellular esterases to produce a polar diol that is well retained within the cells. H9c2 cells were seeded at a density of  $1 \times 10^4$  cells/well in a 96-well plate and  $1 \times 10^6$  cells/well in a 6-well plate. The next day, cells were pretreated with/without NARG (5, 10, and 20 µM) for 24 h followed by incubation with DOX (10 µM) for another 24 h. Then cells were loaded with CM-H2DCFDA (10 µM) as per the manufacturer's protocol for 3 h. Fluorescent intensity was recorded by excitation at 485 nm and emission at 535 nm using a Wallac 1420 Multilabel Counter (Wallac, Turku, Finland). Cells in the 6-well plate were observed under a fluorescence microscope (IX-7, Olympus, Tokyo, Japan) (×200).

### 2.6. Cell morphological analysis

H9c2 cells were seeded at a density of  $1 \times 10^6$  cells/well in a 6-well plate, and the cells were grown overnight at 37°C in a humidified incubator with 5% CO<sub>2</sub>. The next day, cells were pretreated with/without NARG (10 and 20 µM) for 24 h, and then exposed to DOX (10 µM) for another 24 h. After this incubation, cell morphology was examined without/with Wright's Giemsa staining under an inversion microscope (×200).

### 2.7. Measurement of extracellular LDH content, CK levels and cellular GSH-Px activity

H9c2 cells were treated with NARG for 24 h, followed by incubation with 10 µM DOX for another 24 h. After collecting cell culture supernatants extracellular LDH content and CK levels were measured using commercially available colorimetric assay kits respectively. Treated cells were harvested and resuspended in cell lysis buffer (13), supernatants

separated were used for measurement of GSH-Px activity according to the commercially available colorimetric assay kits.

### 2.8. Measurement of intracellular $Ca^{2+}$ concentration

Intracellular  $Ca^{2+}$  concentration ( $[Ca^{2+}]_i$ ) was measured by incubating H9c2 cells with the fluorescent  $Ca^{2+}$  indicator Fura-2/AM using the Multilabel Counter Victor-1420. Briefly, H9c2 cells were seeded at a density of  $1 \times 10^6$  cells/well in a 6-well plate, and the cells were grown overnight at  $37^\circ C$  in a humidified incubator with 5%  $CO_2$ . The next day, cells were pretreated with/without NARG (5, 10 and 20  $\mu M$ ) for 24 h, and exposed to DOX (10  $\mu M$ ) for another 24 h. After this incubation, cells were resuspended in Hanks' solution at a density of  $10^6$ - $10^7$  cells/mL. Trypan blue staining showed a 90%-95% cellular viability rate. A final concentration of 5  $\mu M$  Fura-2/AM was added to the above isolated cell suspensions incubated at  $37^\circ C$  for 35 min, and then were washed with Hank's solution containing 0.1% bovine serum albumin to wash out the residual Fura-2/AM. The cells were resuspended in Hank's solution and incubated for five minutes at  $37^\circ C$  prior to measurements. The basal emission was measured by stimulating the cells with 340 to 380 nm light and recording the emitted fluorescence intensity at 510 nm. In order to calculate  $[Ca^{2+}]_i$ , calibration at high and low  $[Ca^{2+}]_i$  was made after the cells were treated with 0.1% Triton X-100 in PBS, followed by exchanging with calcium-free medium containing 5 mM EGTA in PBS. This produced calcium signals equivalent to saturated calcium and to zero calcium. Calculation of intracellular calcium was made using the following equation (17,18):  $[Ca^{2+}]_i = K_d(R-R_{min})/(R_{max}-R)F_{min}/F_{max}$  where  $K_d$  is the dissociation constant of Fura-2 for  $Ca^{2+}$  and is assumed to be 224 nM at  $37^\circ C$ . R is the ratio of corrected fluorescence at 340 and 380 nm. Rmax is the ratio obtained after 0.1% Triton X-100 treatment. Rmin is the ratio obtained after EGTA treatment. Fmin and Fmax are fluorescent intensity at 380 nm after EGTA and 0.1% Triton X-100 treatment respectively.

### 2.9. Statistical analysis

All data are expressed as mean  $\pm$  S.D. from at least four independent experiments. Differences between mean values of multiple groups were analyzed by Student's t-test. Statistical significance was considered at  $p < 0.05$ .

## 3. Results

### 3.1. NARG protects H9c2 cells from DOX-induced cytotoxicity

H9c2 cells were treated with NARG (5, 10, 20, 40,

and 80  $\mu M$ ) in the absence of DOX for 24 h and then the rates of cell growth inhibition were evaluated. As shown in Figure 1A, NARG at each of these concentrations alone did not cause any apparent cytotoxicity. To analyze the effects of NARG on DOX-induced cytotoxicity in H9c2 cells, cell proliferation was examined after incubation with NARG in the presence of DOX (10  $\mu M$ ). As shown in Figure 1B, NARG (5, 10, 20, 40, and 80  $\mu M$ ) pretreatment provided significant protective effects on DOX-mediated cytotoxicity in a dose-dependent manner at low doses.

To determine whether NARG could protect H9c2 cells from DOX-induced injury, cell morphology was examined without/with Wright's Giemsa staining under an inverted microscope. As shown in Figure 2A, normal cells were seen as spindle-shaped with integral and clear structures (Aa). NARG (10 and 20  $\mu M$ ) alone had no apparent effects on H9c2 cells (Ab and Ac). Treatment with DOX (10  $\mu M$ ) for 24 h leads to alterations in cell shape, which include cell shrinkage starting from the periphery and accompanied by membrane blebbing. DOX also induced rapid changes in the nuclear morphology of H9c2 cells with increased nucleus size and chromatin condensation (Ad). Pretreatment with 10 and 20  $\mu M$  NARG significantly protected the cells from the morphological changes induced by DOX as shown in Figure 2A (Ae and Af). This result is consistent with the morphological analysis using Wright's Giemsa

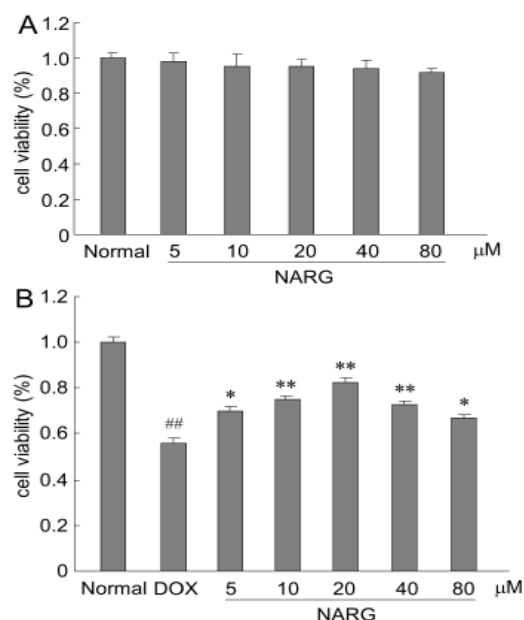


**Figure 1. Effects of NARG on DOX-induced injury in H9c2 cells.** Proliferation of H9c2 cells exposed to NARG in the absence (A) or presence (B) of DOX *in vitro*. Cells were incubated without or with NARG (5, 10, 20, 40, and 80  $\mu M$ ) for 24 h, followed by incubation with (10  $\mu M$ ) DOX for another 24 h. After this incubation, cell viability was determined using the MTT assay. Values represented are means  $\pm$  S.D. ( $n = 6$ ). <sup>##</sup>  $p < 0.01$  compared to the normal group; <sup>\*</sup>  $p < 0.05$ , <sup>\*\*</sup>  $p < 0.01$  compared to DOX group.

staining (Figure 2B).

### 3.2. Determination of cellular ROS

One potential mechanism for DOX-induced cell damage seems to be linked to an increased production of ROS (2,19). Oxidative stress precedes the development of irreversible cell injury after DOX exposure in H9c2 cells. To determine whether pretreatment with NARG mitigated DOX-induced early oxidative stress, cellular ROS contents were measured by incubating the control or drug-treated cells with 10  $\mu$ M CM-H2DCFDA. As shown in Figures 3A and 3B, exposure to DOX without NARG significantly increased fluorescence, indicating that DOX generated oxidative stress. Pretreatment with NARG (5, 10, and 20  $\mu$ M) significantly inhibited the elevated intracellular concentration of ROS compared with DOX treated cells.

### 3.3. Measurement of exellular LDH content and CK levels and GSH-Px activity

The integrity of plasma membranes was determined by monitoring the activity of cytoplasmic enzyme

LDH and CK in the extracellular incubation medium, which represents a common procedure to determine membrane leakage and cellular damage. As shown in Table 1, compared with normal cells, exposure to DOX without NARG, the released amount of LDH and CK was increased for both; the activity of GSH-Px was decreased. Compared with DOX, NARG significantly decreased the amount of released LDH and the content of CK, but the activity of GSH-Px was increased; these results suggest that NARG could prevent cardiomyocytes from DOX-induced toxicity partly by their property of stabilizing cell membranes.

### 3.4. The measurement of the intracellular $Ca^{2+}$ concentration

DOX-mediated alteration of  $Ca^{2+}$  homeostasis is another possible mechanism of cardiotoxicity. Intracellular  $Ca^{2+}$  accumulation is thought to initiate myocardial injury and contractile impairment. In the present study, intracellular  $Ca^{2+}$  levels were determined using the intracellular  $Ca^{2+}$  probe Fura-2/AM. As depicted in Figure 4,  $[Ca^{2+}]_i$  level was quite low in normal cells. Cardiomyocytes exposed to DOX without NARG had

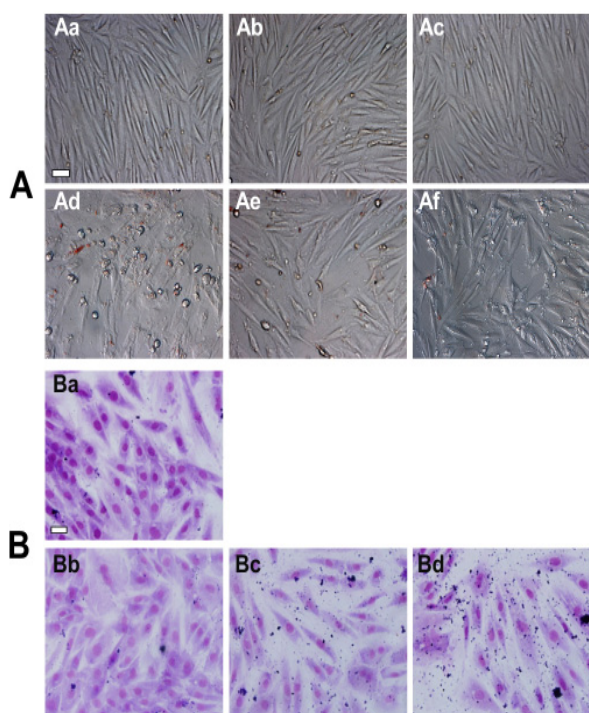


**Figure 2. Morphology of H9c2 cells treated with NARG and DOX.** H9c2 cells were treated without or with (10 and 20  $\mu$ M) NARG for 24 h, followed by incubation with 10  $\mu$ M DOX for another 24 h. Morphology of H9c2 cells was assessed using an Olympus inverted phase contrast microscope ( $\times 200$ ) equipped with a quick imaging system. All images are the same magnification; scale bar = 20  $\mu$ m. (A): images without Wright's Giemsa staining. Aa, control; Ab, 10  $\mu$ M NARG; Ac, 20  $\mu$ M NARG; Ad, 10  $\mu$ M DOX; Ae, 10  $\mu$ M NARG plus 10  $\mu$ M DOX; Af, 20  $\mu$ M NARG plus 10  $\mu$ M DOX. (B): images with Wright's Giemsa staining. Ba, control; Bb, 10  $\mu$ M DOX; Bc, 10  $\mu$ M NARG plus 10  $\mu$ M DOX; Bd, 20  $\mu$ M NARG plus 10  $\mu$ M DOX.

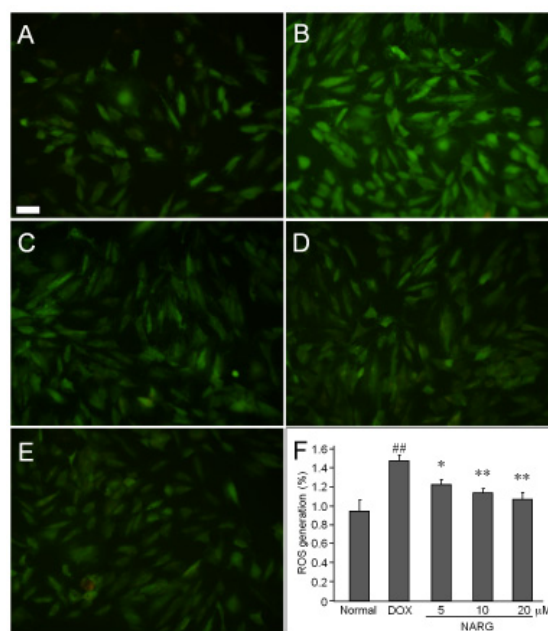


**Figure 3. Effect of NARG on intracellular ROS concentration in H9c2 cells.** H9c2 cells were treated without or with (5, 10 and 20  $\mu$ M) NARG for 24 h, followed by incubation with 10  $\mu$ M DOX for another 24 h. ROS generation was assayed by CM-H2DCFDA (10  $\mu$ M) oxidation-based fluorescence using a fluorescence microscope (magnification,  $\times 200$ ). All images are the same magnification; scale bar = 20  $\mu$ m. (A), control; (B), 10  $\mu$ M DOX; (C), 5  $\mu$ M NARG plus 10  $\mu$ M DOX; (D), 10  $\mu$ M NARG plus 10  $\mu$ M DOX; (E), 20  $\mu$ M NARG plus 10  $\mu$ M DOX. Fluorescent intensity was measured using a microplate reader (F). Signal intensity from six independent experiments was averaged for each condition. <sup>##</sup>  $p < 0.01$  compared to the normal group; <sup>\*</sup>  $p < 0.05$ , <sup>\*\*</sup>  $p < 0.01$  compared to DOX group.

**Table 1. Effects of NARG on excellular LDH content, CK level, and activities of cellular GSH-Px (mean  $\pm$  S.D.,  $n = 5$ )**

Group	Final concentration ( $\mu$ M)	LDH (U/mL)	TCK (U/mL)	GSH-Px (U/mL)
Normal	Equal volume	0.42 $\pm$ 0.02	0.91 $\pm$ 0.01	167.0 $\pm$ 6.6
DOX	10	0.78 $\pm$ 0.10 <sup>##</sup>	1.83 $\pm$ 0.15 <sup>##</sup>	76.6 $\pm$ 9.3 <sup>##</sup>
NARG	5	0.73 $\pm$ 0.06	1.29 $\pm$ 0.14*	98.5 $\pm$ 8.4*
	10	0.60 $\pm$ 0.04*	1.13 $\pm$ 0.02**	114.7 $\pm$ 7.7**
	20	0.59 $\pm$ 0.08*	1.02 $\pm$ 0.02**	127.1 $\pm$ 8.1**

<sup>##</sup>  $p < 0.01$  vs. normal and \*  $p < 0.05$ , \*\*  $p < 0.01$  vs. DOX.

significantly increased concentrations of intracellular  $\text{Ca}^{2+}$  ( $p < 0.01$ ). However, pretreatment with NARG (5, 10, and 20  $\mu$ M) inhibited DOX-induced  $[\text{Ca}^{2+}]_i$  rise in a dose-dependent manner.

#### 4. Discussion

DOX is a widely used chemotherapeutic agent for treatment of various cancers. However, its clinical use is limited by its severe cumulative dose-related cardiotoxicity (20, 21). Although DOX-induced injury appears to be multifactorial, one of the possible mechanisms is cellular damage mediated by generation of ROS (22). DOX-induced cardiotoxicity is associated with the accumulation of DOX in the mitochondria and ROS production (19, 23). The heart is especially susceptible to oxidative damage because cardiomyocytes are rich in mitochondria, the site of basal ROS generation, and are exposed to relatively high oxygen tension compared to other tissues. In normal healthy cells, endogenous antioxidants, such as manganese superoxide dismutase (MnSOD), are able to detoxify basal ROS generation in mitochondria. However, as DOX accumulates and generates ROS, the system becomes easily overwhelmed, and thus, oxidative damage occurs. Therefore, an effective cardioprotective agent perhaps acts partly by preventing DOX-induced ROS production.

Furthermore, ROS may lead to cardiomyocyte apoptosis, endogenous antioxidant system destruction and  $\text{Ca}^{2+}$  overload.  $\text{Ca}^{2+}$  overload can further increase ROS synthesis and is considered an initiating agent of cell apoptosis. Therefore, protection or alleviation of DOX cardiotoxicity can be achieved by reducing oxidative damage, decreasing  $\text{Ca}^{2+}$  overload, and activating endogenous defense systems.

Due to the successful action of DOX as a chemotherapeutic agent, several strategies have been tried to prevent/attenuate the side effects of DOX. Treatment with antioxidants or natural phenolic compounds such as flavonoids has been found to protect against DOX-induced cardiotoxicity *via* radical-scavenging (24), iron-chelating (25), activating endogenous defense systems (26, 27) and regulating intracellular  $\text{Ca}^{2+}$  homeostasis (5).

It has been demonstrated that NARG, a major active flavonoid isolated from *D. rupestris* Hance, did not

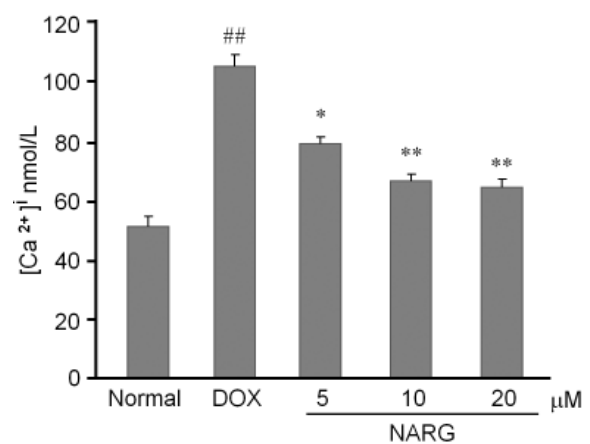


**Figure 4. Effect of NARG on intracellular  $\text{Ca}^{2+}$  concentration in H9c2 cells.** H9c2 cells were treated without or with NARG for 24 h, followed by incubation with 10  $\mu$ M DOX for another 24 h. The intracellular  $\text{Ca}^{2+}$  concentration ( $[\text{Ca}^{2+}]_i$ ) was measured by incubating H9c2 cells with Fura-2/AM. <sup>##</sup>  $p < 0.01$  compared to the normal group; \*  $p < 0.05$ , \*\*  $p < 0.01$  compared to DOX group.

cause apparent cytotoxicity at each investigated low dose alone and could prevent H9c2 cardiomyocytes from DOX-induced toxicity by induction of endogenous antioxidant enzymes *via* phosphorylation of extracellular signal-regulated kinase1/2 (Erk1/2) and nuclear translocation of nuclear factor E2 P45-related factor 2 (Nrf2) (13). NARG could protect against cardiomyocyte apoptosis by modulation of apoptosis-related genes (Bcl-2, caspase-3, and caspase-9) and HO-1 expression (14). Pretreatment with NARG could elevate not only the activities of SOD and catalase (CAT) but also phase 2 metabolizing enzymes such as HO-1 and NAD(P)H: quinone oxidoreductase 1 (NQO1). NARG also could decrease the level of malonaldehyde (MDA) and increase the intracellular reduced glutathione (GSH) level by up-regulating the expression of glutamate-cysteine ligase modifier subunit (GCLM) and glutamate-cysteine ligase catalytic subunit (GCLC) mRNA (13). In this study, we found that pretreatment with NARG increased the activity of GSH-Px.

Efficient detoxification of ROS requires the coordinated actions of various cellular antioxidant enzymes. Accordingly, simultaneous induction of key cellular antioxidant enzymes by NARG in cardiomyocytes appears to be a promising strategy for protecting against oxidative injury and may be an

important mechanism underlying the protective effects of NARG observed in DOX-induced cardiotoxicity. Although the direct antioxidant effects of NARG were not studied. In the present study, we found that compared with DOX, the morphological injury of cells treated with NARG was alleviated, cell viability was increased; the amount of released LDH and CK was significantly decreased; and the content of intracellular  $\text{Ca}^{2+}$  and ROS generation was lowered remarkably. These results suggest that NARG could prevent cardiomyocytes from DOX-induced toxicity by its property of stabilizing cell membranes and reducing ROS generation.

In conclusion, the protection by NARG against DOX-induced oxidative damage and cardiomyocyte death occurs through inhibition of cell death, increased antioxidant activity, decreased cellular calcium overload, and increased mitochondrial function. The findings in our paper of NARG protection against DOX-induced cardiotoxicity conclude that in H9c2 cardiomyocytes NARG is able to prevent DOX-induced oxidative damage and cell death, which is very promising; however, whole animal studies are necessary as the next step to evaluate the ability of NARG to protect the heart from DOX *in vivo*.

#### Acknowledgements

This work was supported by grants from the Natural Science Foundation of Shandong Province (No. Y2007C098) and the Technology Development Planning of Shandong Province (No. 2009GG10002083) of China.

#### References

1. Takemura G, Fujiwara H. Doxorubicin-induced cardiomyopathy from the cardiotoxic mechanisms to management. *Prog Cardiovasc Dis.* 2007; 49:330-352.
2. Kim SY, Kim SJ, Kim BJ, Rah SY, Chung SM, Im MJ, Kim UH. Doxorubicin-induced reactive oxygen species generation and intracellular  $\text{Ca}^{2+}$  increase are reciprocally modulated in rat cardiomyocytes. *Exp Mol Med.* 2006; 38:535-545.
3. Minotti G, Menna P, Salvatorelli E, Cairo G, Gianni L. Anthracyclines: Molecular advances and pharmacologic developments in antitumor activity and cardiotoxicity. *Pharmacol Rev.* 2004; 56:185-229.
4. Gewirtz DA. A critical evaluation of the mechanisms of action proposed for the antitumor effects of the anthracycline antibiotics adriamycin and daunorubicin. *Biochem Pharmacol.* 1999; 57:727-741.
5. Sag CM, Köhler AC, Anderson ME, Backs J, Maier LS. CaMKII-dependent SR  $\text{Ca}^{2+}$  leak contributes to doxorubicin-induced impaired  $\text{Ca}^{2+}$  handling in isolated cardiac myocytes. *J Mol Cell Cardiol.* 2011; 51:749-759.
6. Simůnek T, Stěrba M, Popelová O, Adamcová M, Hrdina R, Gersl V. Anthracycline-induced cardiotoxicity: Overview of studies examining the roles of oxidative stress and free cellular iron. *Pharmacol Rep.* 2009; 61:154-171.
7. Vitelli MR, Filippelli A, Rinaldi B, Rossi S, Palazzo E, Rossi F, Berrino L. Effects of docosahexaenoic acid on  $[\text{Ca}^{2+}]_i$  increase induced by doxorubicin in ventricular rat cardiomyocytes. *Life Sci.* 2002; 71:1905-1916.
8. Bast A, Kaiserová H, den Hartog GJ, Haenen GR, van der Vijgh WJ. Protectors against doxorubicin-induced cardiotoxicity: Flavonoids. *Cell Biol Toxicol.* 2007; 23:39-47.
9. Wu ZY, Li XW. *Flora Reipularis Sinicase. Flora Republicae Popularis Sinicae.* 1977; 65:378-380. (in Chinese)
10. Ren DM, Guo HF, Wang SQ, Lou HX. Separation and absolute configuration assignment of two diastereomeric pairs of enantiomers from *Dracocephalum rupestre* by high-performance liquid chromatography with circular dichroism detection. *J Chromatogr A.* 2007; 1161:334-337.
11. Ren DM, Guo HF, Yu WT, Wang SQ, Ji M, Lou HX. Stereochemistry of flavonoidal alkaloids from *Dracocephalum rupestre*. *Phytochemistry.* 2008; 69:1425-1433.
12. Wang SQ, Han XZ, Li X, Ren DM, Wang XN, Lou HX. Flavonoids from *Dracocephalum tanguticum* and their cardioprotective effects against doxorubicin-induced toxicity in H9c2 cells. *Bioorg Med Chem Lett.* 2010; 20:6411-6415.
13. Han X, Ren D, Fan P, Shen T, Lou H. Protective effects of naringenin-7-*O*-glucoside on doxorubicin-induced apoptosis in H9c2 cells. *Eur J Pharmacol.* 2008; 581:47-53.
14. Han X, Pan J, Ren D, Cheng Y, Fan P, Lou H. Naringenin-7-*O*-glucoside protects against doxorubicin-induced toxicity in H9c2 cardiomyocytes by induction of endogenous antioxidant enzymes. *Food Chem Toxicol.* 2008; 46:3140-3146.
15. Ren D, Lou H, Ji M. Studies on constituents of *Dracocephalum rupestra*. *Chinese Pharmaceutical Journal.* 2005; 40:1695-1696. (in Chinese)
16. Ren DM, Lou HX, Ma B, Ji M. Determination of naringenin-7-*O*-glucoside and eriodictyol-7-*O*-glucoside in *Dracocephalum rupestra* and its different parts by HPLC. *Natural Product Research and Development.* 2003; 15:229-231. (in Chinese)
17. Grynkiewicz G, Poenie M, Tsien RY. A new generation of  $\text{Ca}^{2+}$  indicators with greatly improved fluorescence properties. *J Biol Chem.* 1985; 260:3440-3450.
18. Liao CW, Lien CC. Estimating intracellular  $\text{Ca}^{2+}$  concentrations and buffering in a dendritic inhibitory hippocampal interneuron. *Neuroscience.* 2009; 164:1701-1711.
19. Berthiaume JM, Wallace KB. Adriamycin-induced oxidative mitochondrial cardiotoxicity. *Cell Biol Toxicol.* 2007; 23:15-25.
20. Ferreira AL, Matsubara LS, Matsubara BB. Anthracycline-induced cardiotoxicity. *Cardiovasc Hematol Agents Med Chem.* 2008; 6:278-281.
21. Jones RL, Swanton C, Ewer MS. Anthracycline cardiotoxicity. *Expert Opin Drug Saf.* 2006; 5:791-809.
22. Keefe DL. Anthracycline-induced cardiomyopathy. *Semin Oncol.* 2001; 4:2-7.
23. Salvatorelli E, Guarnieri S, Menna P, Liberi G, Calafiore AM, Mariggio MA, Mordente A, Gianni L, Minotti G. Defective one- or two-electron reduction of the anticancer anthracycline epirubicin in human heart: Relative importance of vesicular sequestration and

- impaired efficiency of electron addition. *J Biol Chem.* 2006; 281:10990-11001.
24. Sadzuka Y, Sugiyama T, Shimoi K, Kinae N, Hirota S. Protective effect of flavonoids on doxorubicin-induced cardiotoxicity. *Toxicol Lett.* 1997; 92:1-7.
25. van Acker SA, van Balen GP, van den Berg DJ, Bast A, van der Vijgh WJ. Influence of iron chelation on the antioxidant activity of flavonoids. *Biochem Pharmacol.* 1998; 56:935-943.
26. Bast A, Kaiserová H, den Hartog GJ, Haenen GR, van der Vijgh WJ. Protectors against doxorubicin-induced cardiotoxicity: Flavonoids. *Cell Biol Toxicol.* 2007; 23:39-47.
27. Crespo I, García-Mediavilla MV, Almar M, González P, Tuñón MJ, Sánchez-Campos S, González-Gallego J. Differential effects of dietary flavonoids on reactive oxygen and nitrogen species generation and changes in antioxidant enzyme expression induced by proinflammatory cytokines in Chang Liver cells. *Food Chem Toxicol.* 2008; 46:1555-1569.

(Received November 19, 2011; Revised February 8, 2012; Accepted February 9, 2012)